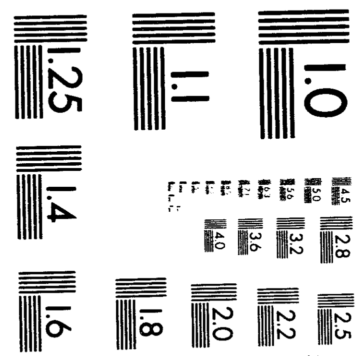

1 of 1

Conf-931079--12

SAND93-1498C

MELCOR Technical Assessment at SNL†

L. N. Kmetyk, T. J. Tautges
Thermal/Hydraulic Analysis Department
Sandia National Laboratories
Albuquerque, NM 87185-5800

1 Introduction

MELCOR [1] is a fully integrated, engineering-level computer code that models the progression of severe accidents in light water reactor (LWR) nuclear power plants, which is being developed at Sandia National Laboratories for the U. S. Nuclear Regulatory Commission (USNRC). The entire spectrum of severe accident phenomena, including reactor coolant system and containment thermal/hydraulic response, core heatup, degradation and relocation, and fission product release and transport, is treated in MELCOR in a unified framework for both boiling water reactors (BWRs) and pressurized water reactors (PWRs). The MELCOR computer code has been developed to the point that it is now being successfully applied in severe accident analyses, particularly in probabilistic risk assessment (PRA) studies.

MELCOR was the first of the severe accident analysis codes to undergo a formal peer review process. One of the major conclusions of the recent MELCOR Peer Review [2] was the need for a more comprehensive and more systematic program of MELCOR assessment. A systematic program of code assessment provides a number of benefits, including:

1. guidance to the code developers in identification of areas where code improvements are needed (such as coding implementation errors in models, inappropriate or deficient models, missing models, excessive numerical sensitivities),
2. documented evidence to external observers, users, reviewers and project management that the code is modelling required phenomena correctly, and
3. increased general public acceptance that the code adequately treats issues related to public safety concerns.

---

†This work was supported by the U. S. Nuclear Regulatory Commission and performed at Sandia National Laboratories, which is operated by the U. S. Department of Energy under contract DE-AC04-94AL85000.

Since the MELCOR Peer Review process identified a need for more code assessment, a number of formal assessment analyses have been completed and documented by Sandia, including:

1. the LACE LA4 containment-geometry aerosol deposition test [3],
2. the FLECHT SEASET natural circulation tests [4],
3. the ACRR ST-1/ST-2 in-pile source term experiments [5],
4. the OECD LOFT integral severe accident experiment LP-FP-2 [6],
5. the Marviken-V ATT-2b and ATT-2 aerosol transport and deposition tests in primary system geometries [7], and
6. PNL ice condenser experiments 11-6 and 16-11 [8].

Results for those analyses have been presented previously [9].

Recent assessment work at Sandia has concentrated on evaluating new code models added in version 1.8.2. Many of these models were developed and incorporated into the code in response to major deficiencies identified by the MELCOR peer review. MELCOR assessment analyses at Sandia (either recently completed or still in progress) whose results will be summarized in this paper include:

1. the ACRR DF-4 fuel damage experiment [10],
2. the SNL and ANL IET direct containment heating (DCH) experiments [11],
3. PWR TMLB' calculations with and without direct containment heating [12], and
4. the ACRR MP-1 late-phase melt-progression experiment.

(Also contributing to code evaluation and assessment are participation in international standard problem (ISP) exercises. SNL has used MELCOR for the TMI-2 standard problem [13], containment hydrogen mixing and stratification experiment HDR T31.5 (ISP23) [14], and core damage tests Phebus B9+ (ISP28) [15, 16], and CORA 13 (ISP31) [17].)

One of the major contributions of this assessment project to the MELCOR effort has been the systematic search for and identification of code features which lead to time step and other numerical dependencies, as summarized in the individual task reports. Nearly all major advances in elimination of these undesirable features during the last year are the result of these systematic studies. Many of the numeric sensitivities have been traced to code problems that would not be readily detected in the single, isolated calculations that are typical of many user applications.

In addition, a number of user guidelines on input modelling and on the adequacy and applicability of default parameter settings are being generated, with details contained in the individual assessment reports. In some cases, these will be included in the preliminary users' guide now being prepared. In other cases, the end result is a change in the code documentation or changes to the default variable setting in the code; this latter option may be more effective in the long term because it eliminates the need to document when and why the user should override default settings.

2 ACRR DF-4 BWR Fuel Damage Experiment

MELCOR has been used to model the ACRR DF-4 damaged fuel experiment; DF-4 provided data for early-phase melt progression in BWR fuel assemblies, particularly for phenomena associated with eutectic interactions in the BWR control blade and zircaloy oxidation in the canister and cladding. [10] In addition to comparison with test data, the results of the basecase MELCOR calculation were compared to results of DF-4 analyses performed using 4 more mechanistic codes (APRIL.MOD3, BWRSAR/DF4, MELPROG-PWR/MOD1 and SCDAP/RELAP5/MOD2).

Figure 2.1 presents control blade and clad temperatures at the 36.8cm core elevation predicted by MELCOR, compared to test data and to other code results, as an example of the results obtained for the ACRR DF-4 assessment analyses. The basecase model underpredicted control blade temperatures in the early parts of the experiment by almost 200K but, in later stages of the experiment when all the core damage was taking place, calculated control blade temperatures corresponded almost exactly to measured values. Control blade failure times in most of the test bundle were predicted very well compared to experimental data. Cladding temperatures were predicted almost exactly compared to experimental data at all times and at all levels except for the uppermost axial level; MELCOR overpredicted temperatures in the uppermost axial levels by close to the same amount (~250K) as other codes did during the middle of the experiment, leading us to believe that the power coupling relationship did not predict power coupling well in this part of the core. Fuel failure times calculated by MELCOR corresponded closely to experimental data. Calculated canister temperatures were also very close to experimental data, after correcting this data for the time and temperature lags associated with the slow-response thermocouples used for the canister.

Material distributions for the melting and relocation portions of the experiment very clearly show the effect of modelling the B_4C-stainless steel eutectic interaction in the control blade. This reaction resulted in the first control blade failure being calculated to occur around 7450s, which was within 10s of the first observed failure in the experiment. Eutectic dissolution of the canister wall was also evident in the calculated material response and was responsible for the calculated failure of lower portions of the canister; evidence of canister failure was seen in the postirradiation examination (PIE) of the DF-4 test bundle.

The material distributions also showed clearly that, in the MELCOR calculations, core materials relocated by axial level and not by component. That is, all components at a single axial level (fuel, clad, canister and control blade) melted and relocated before significant component relocation at other levels. This behavior could be affected by code input. For example, the default candling heat transfer coefficients resulted in the control blade material refreezing quite close to the axial location from which it melted. Behavior would be quite different if the control blade materials were allowed to candle to the bottom of the test bundle, as they did during the DF-4 test. These results are important when considering the possibility of reactivity excursions due to control poison relocation without accompanying relocation of fuel material.

Table 2.1 compares the total hydrogen generation calculated by MELCOR to both test data and to results from other code analyses of this experiment. The amount of hydrogen production calculated by MELCOR was 36.4gm, which was within the amount derived from the PIE (38.0±4.0gm). MELCOR calculated the autocatalytic oxidation reaction to begin sooner than was measured, and predicted 5gm of hydrogen produced before the autocatalytic

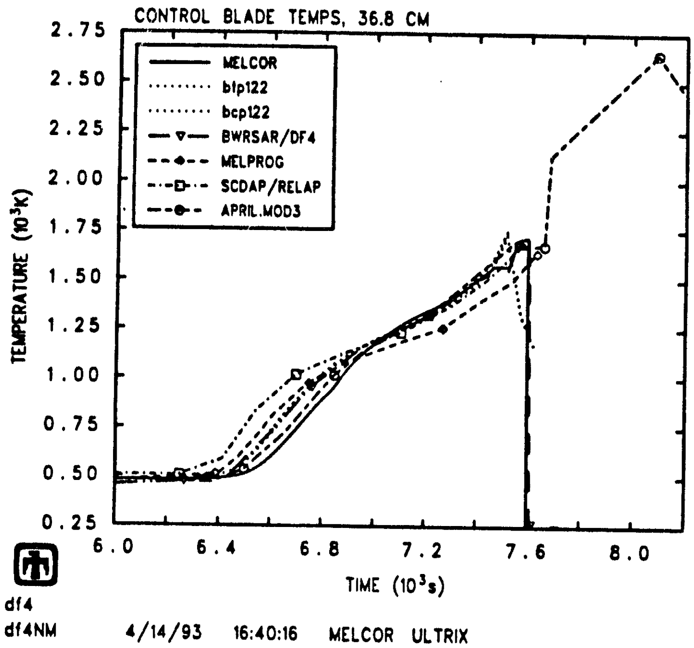

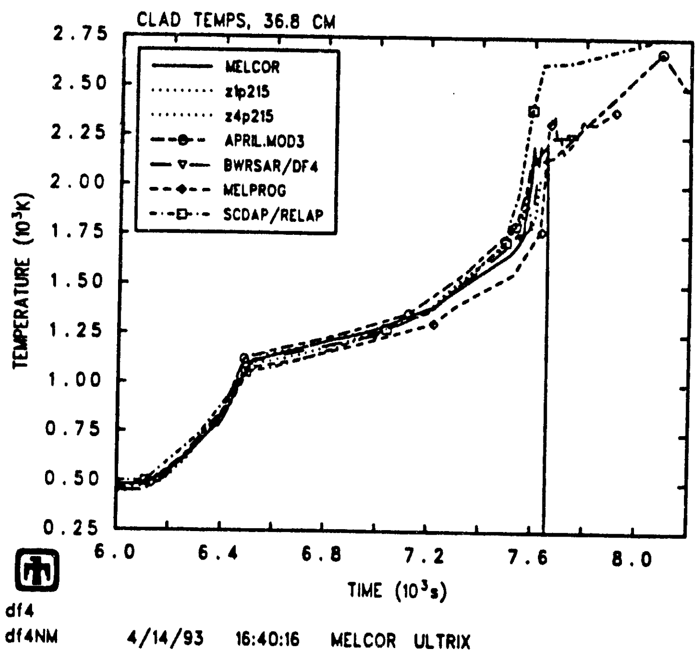

Figure 2.1. ACRR DF-4 Control Blade (top) and Clad (bottom) Temperatures at 36.8cm Elevation Predicted by MELCOR, Compared to Test Data and to Other Code Results

Table 2.1. ACRR DF-4 Total Hydrogen Production Predicted by MELCOR, Compared to Test Data and to Other Code Results

	Total H_2 (gm)
Experiment	33-40
Code	
MELCOR	36.4
APRIL	37.5
MELPROG	51.0
SCDAP/RELAP5	43.0

stage, compared to no hydrogen production measured during that time; other codes predicted early hydrogen production and early transition to the autocatalytic stage as well.

A large number of sensitivity studies were performed on MELCOR input parameters, most of which were in the core (COR) package but also some in the heat structure (HS) and control-volume thermal/hydraulics (CVH) packages. A study which deactivated the eutectics model showed clearly the benefits of using this new model, as deactivating it predicted much different behavior of the B_4C and did not show any canister dissolution. Hydrogen production without the eutectics model was well below both the measured and the MELCOR basecase values. A sensitivity study which varied the eutectic temperature of the B_4C-stainless steel reaction by $\pm 50K$ showed little variation of results. A study which used the default heat structure boundary fluid temperature option (which uses bulk atmosphere temperature instead of local dT/dz temperatures for calculating heat transfer between the core and its boundary heat structures) resulted in much earlier component failure and poorer temperature agreement with the experimental data; this study showed the usefulness of the new HS boundary fluid temperature option (which uses local dT/dz temperatures for calculating heat transfer between the core and its boundary heat structures instead of the control volume bulk atmosphere temperature). A study on minimum oxide shell thickness and two other core material relocation parameters in the COR package showed no variation in results until the critical minimum thicknesses for intact zircaloy and stainless steel were set to zero; then the final core material configuration showed the fuel pellet stacking observed in the PIE, but did not relocate any of the ZrO_2 that resulted from cladding oxidation. Other studies showed sensitivities to zircaloy properties, COR component view factors, allocation of canister mass to either the canister or canister-b component (*i.e.*, canister next to the clad or canister next to the control blade), candling heat transfer coefficient, COR and CVH nodalization, and slight sensitivity to COR and overall time steps. No sensitivities were found to minimum component mass, B_4C oxidation modelling, HS outer boundary temperature, and the machine used to run the problem.

This task resulted in improvements to the COR dT/dz model, the model which calculates axial temperature gradients in the core fluid, in particular the addition of the HS boundary fluid temperature option. Several other code errors were uncovered and corrected during this analysis.

3 IET Direct Containment Heating Experiments

The MELCOR computer code has been used to analyze several of the IET direct containment heating experiments done at 1:10 linear scale at Sandia and at 1:40 linear scale at Argonne National Laboratory. [11]

Most input parameters in our MELCOR model were not separately adjusted in each of our IET analyses to best match data for individual experiments. Instead, the basic CVH/FL/HS model was kept the same for all IET experiments analyzed, and a single set of debris source, distribution and interaction time parameters was used for all the SNL/IET experiments analyzed. The only test-specific changes made were to set the initial pressures, temperatures, gas composition, and liquid pool heights to match individual experiment initial conditions. The characteristic times for settling of debris in the control volume atmospheres onto floor heat structures were based upon free-fall times, and therefore proportional to the volume heights and constant in the various tests. The characteristic oxidation and heat transfer times were assumed to depend primarily on parameters such as average airborne or deposited particle concentrations, which in a given geometry should be approximately constant for identical melt debris and blowdown steam sources such as used in the tests analyzed. The characteristic times for oxidation and heat transfer of debris in the control volume atmospheres, as well as a characteristic time for oxidation of debris deposited on heat structures, were selected after a number of iterations in sensitivity studies as giving reasonable agreement with test data. Note that there is no reason to assume that the debris source and interaction input parameter set used in our reference analyses is unique (*i.e.*, the only set to provide reasonable agreement with the selected test data). It is also not guaranteed that the iterative procedure followed results in an input parameter set that yields the best agreement with data, or agreement with data for the "correct" reasons (*i.e.*, representing the actual behavior). For example, freezing some of the parameter values early in this iterative process undoubtedly affected the values assumed for other parameters. Further, experiment ambiguities may have led to incorrect modelling assumptions which would also affect the values chosen for various parameters.

Figure 3.1 gives vessel pressures predicted by MELCOR for the 1:10-scale IET experiments analyzed, compared to test data, as an example of the results obtained for the DCH assessment analyses. The results of the MELCOR reference calculations for the Surtsey 1:10-scale tests correctly reproduce the subdivision of the pressure response into two major families, caused by the effect of hydrogen combustion, as seen in the test data, with a peak pressure rise of ~100kPa due to HPME and an additional pressure rise of ~150kPa due to hydrogen combustion (IET-3, IET-4, IET-6 and IET-7). The results also correctly reproduce the lack of any significant effects of presence *vs* absence of pre-existing hydrogen (IET-6 and IET-7 *vs* IET-3 and IET-4) or presence *vs* absence of basement condensate water (IET-4 and IET-7 *vs* IET-3 and IET-6).

The hydrogen production and combustion calculated by MELCOR is generally in reasonable agreement with test data. It is difficult to quantitatively compare the measured and calculated hydrogen production and combustion because of the basic assumption made by the experimenters that all oxygen depletion was due to reaction with hydrogen and that debris reacted only with steam, not with free oxygen, which is the opposite of the MELCOR assumption that reaction of metals with free oxygen occurs preferentially to oxidation with steam. Table 3.1 therefore gives pairs of values for the hydrogen production and combustion calculated by MELCOR, presenting both the actual amounts of hydrogen calculated to be produced by HPME steam/metal reactions and burned, and the amounts of hydrogen produced and burned that

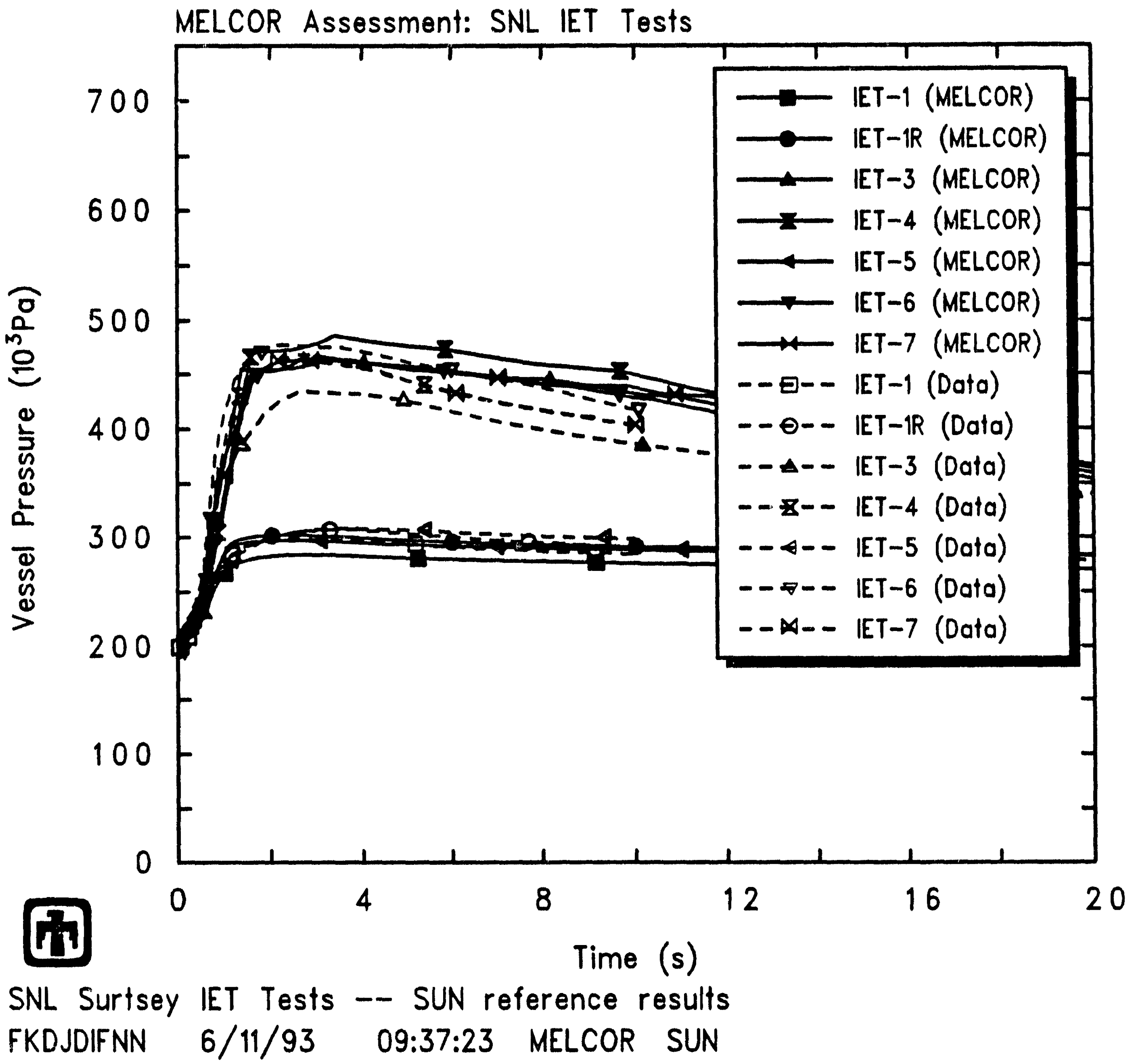

Figure 3.1. SNL/IET Vessel Pressures Predicted by MELCOR, Compared to Test Data

Table 3.1. SNL/IET Hydrogen Production and Combustion Predicted by MELCOR, Compared to Test Data

Experiment	Hydrogen (gm-moles)					
	Produced			Burned		
	Data†	MELCOR¶	MELCOR‡	Data†	MELCOR¶	MELCOR‡
IET-1	233	286	266	3	0	4
IET-1R	248	266	267	11	0	28
IET-3	227	232	352	190	188	313
IET-4	303	243	361	240	209	332
IET-5	319	240	313	53	0	91
IET-6	319	236	354	345	218	307
IET-7	274	229	351	323	223	350

†from gas grab bottle samples at 30min
¶actual end-of-calculation values at 20s
‡calculated from initial and final oxygen and hydrogen moles
assuming only steam/metal reactions

would be calculated using the initial and final oxygen and hydrogen moles from the MELCOR analyses in the same formulae as in the experiment data analysis. The two sets of MELCOR values differ by twice the number of moles of O_2 consumed by direct metal/oxygen reactions.

Overall, the "correct" answers are likely to lie somewhere between the two limiting assumptions. It is unlikely that there is no oxidation of metal with free oxygen at all (as assumed in the experimental analysis protocol). However, MELCOR would be expected to exaggerate the relative degree to which metal oxidizes with free oxygen *vs* with steam. This is partly because of the hierarchical assumptions in the MELCOR FDI/HPME/DCH model. Also, in the experiment the debris transport probably lags the steam/hydrogen mixture flow, so that in the tests not much of the debris gets to see much oxygen; in the MELCOR model the debris is immediately transported to its ultimate distribution (within a user-specified time period, in this case 1s) while the steam blowdown is modelled "normally" as a transient process taking several seconds. The debris is thus more likely to see oxygen in the MELCOR calculation.

The hydrogen combustion observed in these tests could not be calculated using the default burn package input, because the default ignition criteria are never satisfied in these experiments. Instead, we set the hydrogen mole fraction ignition criterion in the absence of igniters to 0, which (in the absence of CO) also gives a combustion completeness correlation value of 0; in addition, burns were suppressed in all control volumes except the vessel dome. This particular combination of input was found to produce reasonable agreement with test data in all cases. A combustion completeness of 0 prevents the burning of any pre-existing hydrogen, but allows burning of any additional hydrogen generated during the HPME. Suppressing burns except in the dome mimicked the experimental behavior of a jet flame burning at the outlet from the subcompartments to the dome; because little or no hydrogen was generated by debris oxidation in the dome in our analyses, only hydrogen advected into the dome from the subcompartments burned, and only on the time scale over which it was advected into the dome.

Most of our calculations were run with control volume flow areas reduced from their default values by factors ≥10, to enhance convective heat transfer from the control volume atmospheres to the heat structure surfaces. (Note that changing control volume flow areas does not affect flow path calculations at all.) This was done for two reasons:

First, preliminary calculations showed that the flow through the system was primarily that associated with steam blowdown only. The MELCOR HPME/DCH model does not model transport of debris between and through volumes but instead deposits the debris directly at its ultimate destination, using the same time-dependent deposition in all volumes regardless of their distance from the debris source. Thus, instead of debris being transported into an "upstream" volume with the blowdown steam and the resultant additional heating adding to the driving force pushing flow further "downstream", the MELCOR logic does not represent this additional driving force and in contrast has debris appearing "upstream" and heating the atmosphere in upstream volumes, if anything contributing a retarding force to the expected flow. This results in lower velocities than the transient HPME blowdown actually occurring in the experiments. Decreasing volume flow areas resulted in increased volume velocities more characteristic of the turbulent conditions that might be expected during HPME.

In addition, the MELCOR HPME/DCH model does not account for any radiation directly from airborne debris to surrounding structures (or from deposited debris directly to atmosphere). Although radiation heat transfer was included in the MELCOR input model, there is little or no calculated atmosphere-structure radiation heat transfer early in these transients, because MELCOR only considers radiation heat transfer for steam and/or CO_2 in atmospheres. In most of the experiment simulations there is very little steam present early in the transient, because any blowdown steam is consumed in debris oxidation soon after arrival, and very little CO_2 present at all. The lack of steam and/or CO_2 in the atmosphere would if anything enhance radiation heat transfer from airborne debris to structures because there would be little absorption in the intervening atmosphere. Hand calculations indicate that this could be a significant heat transfer mechanism early in the transient. Because there is no way in MELCOR to model this effect, too much energy may be deposited in the atmosphere by the airborne debris; because there is no convenient way to enhance atmosphere-structure radiation heat transfer in general, we relied on increasing convective heat transfer instead to help remove that energy.

Sensitivity studies were done on a number of input parameters affected by experiment uncertainties, such as the steam blowdown rate and the debris temperature specified. The time period over which melt injection was specified to occur was varied, and the time-dependence of the melt addition in the MELCOR input was adjusted to match the rate of pressure and temperature increase in the vessel. The majority of our MELCOR analyses simply specified the original thermite charge mass, neglecting both the retention of any debris in the melt generator and the addition of any debris due to melting, vaporization, ablation, and/or oxidation; to determine the effect of the injection mass source uncertainty, calculations were done varying the total melt mass input. In these IET analyses, the debris distribution in our MELCOR input was based on test data but, in most plant analyses, there will be no equivalent data set providing guidance on HPME melt distribution; to evaluate the effect of the debris distribution assumed on the overall DCH behavior calculated, calculations were done in which various debris distribution patterns were assumed. The effects of varying the characteristic debris interaction times were also investigated.

In the HPME/DCH model originally added to MELCOR, any debris immediately deposited onto a heat structure or later settled onto a heat structure essentially left the problem; there was no subsequent interaction of any kind for that debris, except for decay heating of the structure surface. During this DCH assessment, this was identified as a major potential problem area, especially given MELCOR's emphasis on mass and energy conservation. For example, the lack of any thermal interaction of debris with structures could adversely affect the ability to correctly predict late-time revaporization of volatile fission products. Also, the lack of any oxidation of deposited debris meant that the total amount of hydrogen produceable during HPME was very highly dependent on the user-specified initial debris distribution and on the characteristic settling time constants - any debris deposited or settled could not continue to generate hydrogen through further oxidation, regardless of oxygen and/or steam availability or debris temperature and/or amount. Therefore two effects were added to the original HPME model: heat transfer to the structure surface from deposited hot debris, and the continued oxidation of the deposited debris. With these input and coding modifications, HPME debris deposited on structures now can continue to affect the overall system response through several potential interactions.

Several counterpart tests to the IET direct containment heating experiments done at Sandia at 1:10 linear scale were performed at ANL at 1:40 linear scale, in an experimental program to investigate the effects of scale on DCH phenomena. The results of the 1:40-scale IET experiment MELCOR simulations were generally inconclusive. The vessel pressures predicted in our SNL and ANL counterpart-test calculations scaled very well when both the geometry and the characteristic interaction times in the FDI HPME input were scaled, but the test data showed a number of non-scaled effects. In particular, the results of both our own, limited review of the facility and data scalability and of our ANL test simulations indicate that the DCH energy-transfer efficiency is greater at smaller scale, that there is less pressurization due to hydrogen combustion at smaller scale, and that there appears to be a greater effect of pre-existing hydrogen in the ANL 1:40-scale tests than in the counterpart SNL 1:10-scale tests.

The reference MELCOR calculations for the 1:10 linear scale IET experiments have been compared to similar calculations done with the CONTAIN code, when available. The CONTAIN DCH model is quite different from the MELCOR FDI/HPME DCH model, being a more detailed, more mechanistic treatment rather than a more parametric approach. Despite these differences, the results obtained with the two code models are generally quite similar.

Several calculations have been done to identify whether any numeric effects exist in our IET direct containment heating assessment analyses, producing either differences in results on different machines or differences in results when the time step used is varied. The reference calculations were run, using the same code version, on an IBM RISC-6000 Model 550 workstation, on an HP 755 workstation, on a SUN Sparc2 workstation, on a CRAY Y-MP8/864, and on a 50MHz 486 PC. There is generally excellent agreement among results generated on these various hardware platforms. The SUN and PC were always slowest in run time required; the IBM, HP and Cray were all significantly faster with the HP the fastest for these analyses. In addition, otherwise identical calculations were run on a SUN Sparc2 workstation with both the user-input maximum allowed time step and the initial time step size for HPME initiation simultaneously reduced by factors of 2, 10, 20 and 100 from the basecase values. The results showed about half of the analyses fully converged for all these time steps, with the other half demonstrating convergence with reduced time steps.

4 Surry TMLB' with and without DCH

As part of the MELCOR Peer Review process [2], Sandia performed and presented a demonstration calculation of a Surry station blackout (TMLB') accident with MELCOR. This was the first fully-integrated PWR severe accident calculation performed with the code (since the earlier TMI analysis only included in-vessel phenomena). That calculation was done using the release version of MELCOR 1.8.1. The calculation has been rerun with the release version of MELCOR 1.8.2, allowing direct comparison of predicted results for the same problem. That analysis also has been used as a standard test problem to investigate problems identified by the Peer Review (*e.g.*, lack of pressurizer draining prior to vessel breach) and to evaluate the impact on the results of model improvements and extensions (for example, adding the CORSOR-Booth fission product release model) and of new models (such as radial debris relocation, material eutectics interactions, and direct containment heating due to high pressure melt ejection).

No input changes were required between running with the release versions of MELCOR 1.8.1 and 1.8.2. Input changes made in the basecase model to take advantage of new models and/or upgraded models included using step functions in valve area-*vs*-time tables, and enabling the new eutectics model (not used as the default); the new debris radial relocation model is enabled by default. Other input changes for various sensitivity studies included specifying high-pressure melt ejection debris distribution and interactions, varying the fission product release model option, varying the interfacial momentum exchange length in some flow paths, and changing in-vessel falling debris heat transfer parameters.

The results of the same transient run with MELCOR 1.8.1 and 1.8.2 show generally very similar early-time behavior, for the steam generator secondary inventory boiloff, for the pressurizer filling and venting through the PORV, and for the core uncovery and initial clad failure and gap release. The vessel was calculated to fail ~1hr earlier by MELCOR 1.8.2 than by 1.8.1; of that difference, ≥0.5hr was due to correcting the "levitating water" problem diagnosed and corrected during our LOFT LP-LP-2 MELCOR assessment [6], while ≤0.5hr was due to incorrect failure of the blocked core plate in the MELCOR 1.8.1 analysis (corrected in 1.8.2). More hydrogen was generated in-vessel in the MELCOR 1.8.2 analysis than in the MELCOR 1.8.1 analysis, but the total hydrogen generated (adding together in-vessel and in-cavity production) by the two code versions was within 5%. There was very little change in calculated containment response, with a pressure spike at vessel breach shifted in time due to the different vessel failure times, but the same long-term pressure and temperature response predicted by both MELCOR 1.8.1 and 1.8.2. (Note that this direct comparison did not use the new direct containment heating model added in MELCOR 1.8.2, but even with that model enabled there was simply an increase in the containment pressure spike at vessel failure, and no other significant long-term differences in predicted system response.)

During the MELCOR peer review [2], questions were raised concerning the failure of the pressurizer to drain until the time of vessel failure and subsequent primary system depressurization in the MELCOR 1.8.1 Surry TMLB' demonstration calculation; there was general agreement that this appeared to violate physical intuition, and might reflect a code problem. In particular, concern was expressed by members of the peer review committee that the failure of the pressurizer to drain was a result of the inadequacy of the momentum exchange model in MELCOR, leading to an incorrect two-phase countercurrent flow limit (CCFL). In response to this problem (and to other concerns), a number of modifications were made to the code including treating the momentum exchange length as a separate variable from the inertial length, defaulted to the buoyancy force characteristic dimension; user input can be used to override the default if desired. As part of evaluating the current momentum exchange model, the Surry TMLB' analysis which originally highlighted the pressurizer drainage problem was rerun with input appropriate to the new interfacial momentum exchange model in MELCOR, in a number of sensitivity study calculations. The results of this sensitivity study, presented in Figure 4.1, indicate that the ability of the user to change the interfacial momentum exchange length through input added in MELCOR 1.8.2 obviously allows wide variation in countercurrent flow limits and associated pressurizer drainage rates, but the question of the "correct" value to use remains open.

Another code model added in MELCOR 1.8.2 is a debris radial relocation model. Previous versions of MELCOR would predict each radial ring in the core package model responding independently, with artificial "stacking" of debris columns often observed. This new model was added to relocate molten and/or particulate debris between rings (and axial levels), based upon hydrostatic head equilibration. Sensitivity study results for the Surry TMLB' sequence show more coherent behavior among rings when the debris radial relocation model is enabled. There is no effect on early core heatup or initial clad failure and gap release, but a slightly faster core damage progression and earlier lower head penetration failure (at 11,219s with the debris radial relocation model, *vs* 12,531s with that model disabled).

The capability to model a variety of material eutectics interactions (such as inconel and zircaloy, zircaloy and stainless steel, B_4C and stainless steel, zircaloy and Ag-In-Cd, UO_2 and ZrO_2, and B_4C and zircaloy) was also added to the core package modelling in MELCOR 1.8.2. Earlier versions of MELCOR treated each material melting as a separate process, although there was coding for a specified fraction of solid material to be relocated by molten Zr or steel, to represent dissolution of UO_2 and/or ZrO_2 in melts; the new model has a better treatment of the dissolution of solid material by eutectics melts, based on phase equilibrium and dissolution rate limits, proceeding sequentially as determined by a solid dissolution material hierarchy.

Using the new eutectic materials interaction model generally had only a small effect on the results for the Surry TMLB' station blackout sequence. Both earlier core support plate failure (11,178s *vs* 11,675s) and earlier vessel lower head penetration failure (11,219s *vs* 11,685s) were calculated when the model was enabled, but the difference is quite small ($\leq$500s). The biggest difference found was in the lower plenum structural response. Without the eutectics interactions modelled, most ($\sim$80%) of the steel structure in the lower plenum melted and fell into the cavity; the behavior predicted by MELCOR 1.8.2 with the eutectics interactions not modelled was very similar to the results previously obtained using MELCOR 1.8.1. With the eutectics interaction model enabled, Zr and stainless steel debris in the lower plenum melted at lower temperatures and flowed to the cavity somewhat sooner, with less heating of the lower plenum steel structure due to the lower melt temperature and shorter residence time of the debris; thus, most ($\sim$70%) of the lower plenum structure remained in the vessel throughout the entire transient period analyzed. The larger amount of stainless steel transferred to the cavity in the case without the eutectics interactions modelled resulted in a thicker metallic layer in CORCON existing for a longer time period, and the increased concrete ablation then resulted in slightly higher ($\leq$5%) containment pressures at late times.

A set of MELCOR Surry TMLB' assessment analyses were run with different fission product release model options enabled in MELCOR, as a sensitivity study on fission product source term. These include the CORSOR and CORSOR-M models, each with and without a surface-volume correction term, and the new CORSOR-Booth model with low- and high-burnup coefficient

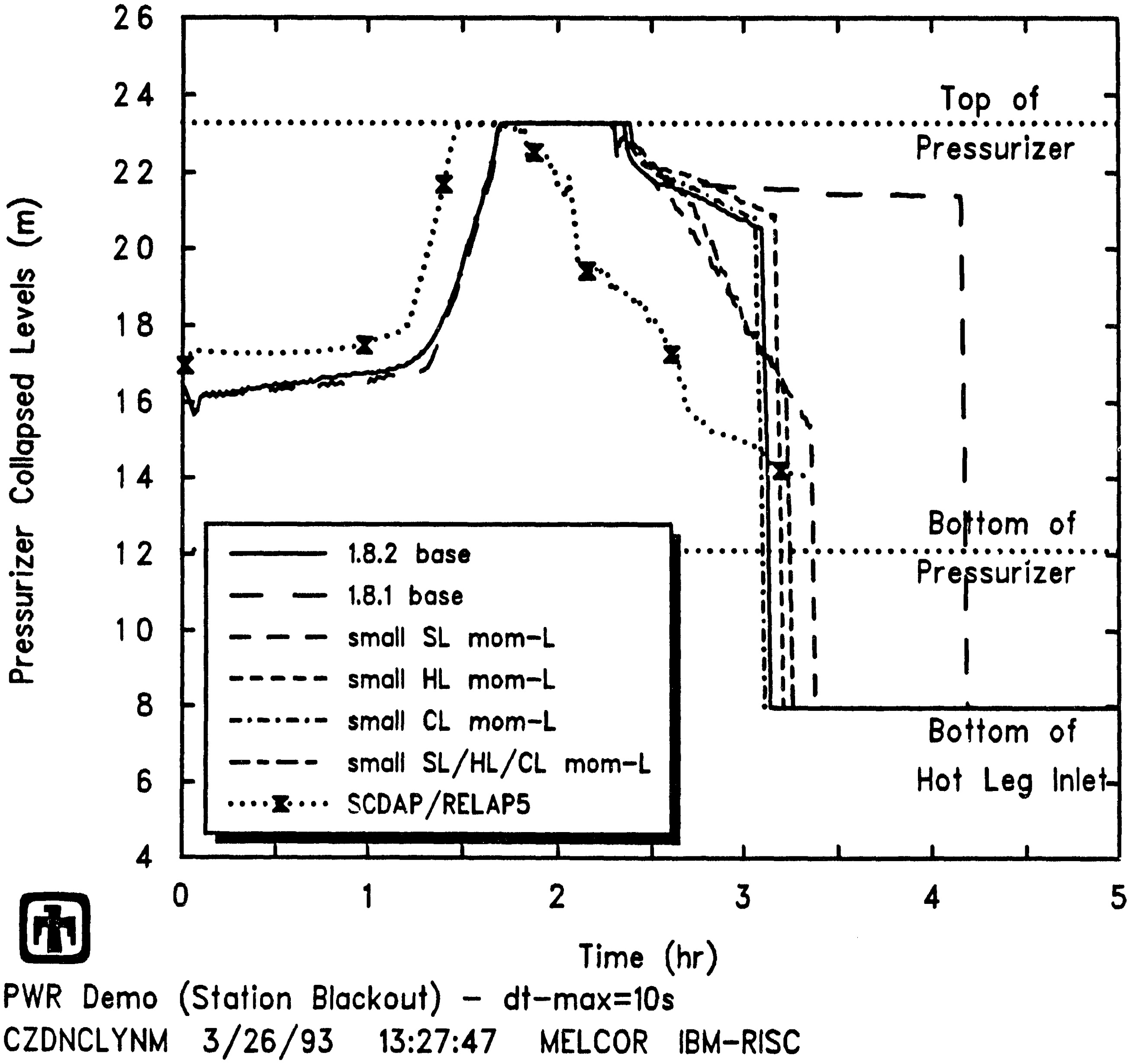

Figure 4.1. Pressurizer Liquid Levels for Surry TMLB' - Interfacial Momentum Exchange Length Sensitivity Study

Table 4.1. Total Source Terms for Surry TMLB'– CORSOR Options Sensitivity Study

Class	Radionuclide Release (% Initial Inventory) CORSOR	CORSOR (S/V)	CORSOR-M	CORSOR-M (S/V)	CORSOR-Booth high-burnup	CORSOR-Booth low-burnup
1 (Xe)	99.987	99.256	98.782	98.921	96.715	98.937
2 (Cs)	102.58	102.26	102.03	100.90	99.515	102.18
3 (Ba)	28.584	37.786	30.928	30.999	28.737	22.270
4 (I)	66.600	60.284	56.718	73.219	47.065	49.777
5 (Te)	52.317	90.106	92.208	98.562	87.669	67.553
6 (Ru)	0.2547	0.2765	0.0005	0.0012	1.8352	2.0470
7 (Mo)	3.7796	5.2802	2.2908	2.2279	2.1838	0.9152
8 (Ce)	0.0059	0.0067	0.0011	0.0015	0.0029	0.0025
9 (La)	0.2353	0.3303	0.1732	0.1808	0.2064	0.1360
10 (U)	0.0896	0.0503	0.0253	0.0584	0.0080	0.0065
11 (Cd)	31.129	27.881	0.8048	2.4303	25.553	20.817
12 (Sn)	33.252	52.188	10.716	36.226	35.853	22.619

sets, for a total of six possible variations (although obviously only the high-burnup version of the CORSOR-Booth model should apply to most plant analyses). The final amounts of each class predicted to be released by the end of the calculated transient period (90,000s or 25hr) are given in Table 4.1, as a percent of inventory initially present in the core. (Note that these amounts consider only the release of radioactive forms of these classes, and not additional releases of nonradioactive aerosols from structural materials.)

In-vessel, the CORSOR and CORSOR-M options result in similar releases of the Xe, Cs and I volatiles. The CORSOR expression and constants give higher releases for many classes (Ba, Ru, Mo, Ce, La, Cd and Sn), while the CORSOR-M expression and constants produce significantly higher release of Te, with no release at all of Mo, La or Cd. The new CORSOR-Booth model predicts lower releases for the most volatile species (Xe, Cs and I), as well as for Ba, Te and U, than either of the older CORSOR options, while the releases of some other species are intermediate between the higher CORSOR and lower CORSOR-M predictions. The effects of using various CORSOR options are less evident in the total-release comparisons, because the later ex-vessel release can somewhat compensate for in-vessel differences.

Using any of the CORSOR options, the total release of Class 2 (Cs) calculated is greater than the initial inventory present. This is due to a coding problem in the default radionuclide class mapping MELCOR: the VANESA code, which is used to calculate the ex-vessel release within MELCOR, considers iodine to be released as CsI; since there is no separate CsI class in these MELCOR calculations, MELCOR assumes that CsI release to be a Class 2 (Cs) release.

Based upon physical insight, the Class 4 release should closely resemble the Class 1 and 2 results. (The default class mapping has been corrected in subsequent code versions.)

In two cases in this source-term sensitivity study (using CORSOR without the S/V term and using the low-burnup form of CORSOR-Booth), there was no high-pressure melt ejection of debris immediately following lower head penetration failure, but instead debris falling into the lower plenum water pool was sufficiently quenched that it remained in the lower plenum for ~2,000-3,000s before reheating sufficiently (to melt) that it could fall into the cavity. The delay in debris ejection in these two cases affects the releases in the lower plenum, because there is more debris in the lower plenum for a longer period of time to contribute to the released source term. The delay in debris ejection in these two cases also affects the melting and ejection of the structural steel mass in the lower plenum, as illustrated in the upper left of Figure 4.2, because there is more debris in the lower plenum for a longer period of time to heat the structural material there. The increased retention of steel mass in the lower plenum in the other four calculations resulted in a smaller, thinner metallic layer in the cavity, which was completely oxidized by the end of the transient, as indicated in the upper right of Figure 4.2. The VANESA code [18], which is used to calculate ex-vessel releases in MELCOR, has no provision for a disappearing metallic layer; therefore, as the metallic layer in the cavity goes to zero, the releases of radionuclide species associated with that layer (*i.e.*, Te, Ru, Sb, Sn, and unoxidized Zr and Fe) begin growing exponentially. This is shown in the lower half of Figure 4.2 for two of these radionuclide species. The effect is not pronounced for Te, because most of that species mass had been released prior to the metallic layer vanishing; however, the release of other species, such as Sn, is significantly in error. This problem is inherent in the VANESA formulation itself, not in MELCOR, but is more likely to be encountered with MELCOR 1.8.2 than with MELCOR 1.8.1 because of the increased likelihood of more retention of lower plenum structural steel in-vessel.

The new direct containment heating model added in MELCOR 1.8.2, which models high pressure melt ejection from the vessel into containment, also has been used in these PWR TMLB' analyses. These Surry TMLB' DCH analyses relied heavily on modelling insights and code improvements from the MELCOR DCH assessment analyses of the IET experiments [11].

Initial calculations showed a rapid, brief pressure and temperature spike in containment immediately upon high-pressure melt ejection and direct containment heating. The effect was not extremely pronounced, because only ~15% of the available core material was predicted to be ejected during the high-pressure melt ejection phase in our reference Surry TMLB' calculation.

The amount of melt in the lower plenum at failure is a concatenation of early-time core damage, core plate failure criteria, falling debris heat transfer and possible quench in the lower plenum, and lower head penetration heat transfer and failure criteria. The core plate and bottom head penetration failure temperatures, and the falling debris and lower head penetration heat transfer coefficients were all set to their default values in the MELCOR reference calculation. Sensitivity studies were done varying some of these parameters, but there is little data available for these phenomena, either for evaluation of the MELCOR models' adequacy or for guidance on the values to use for the various input parameters controlling predicted response. In addition, calulations were done in which the peaking factors used were adjusted until ~60% of the available core material was predicted to be ejected during the high-pressure melt ejection phase; this was not to represent "correct" values for core power peaking, but simply to allow a comparison of DCH behavior in otherwise similar calculations with different amounts of high-pressure melt ejection.

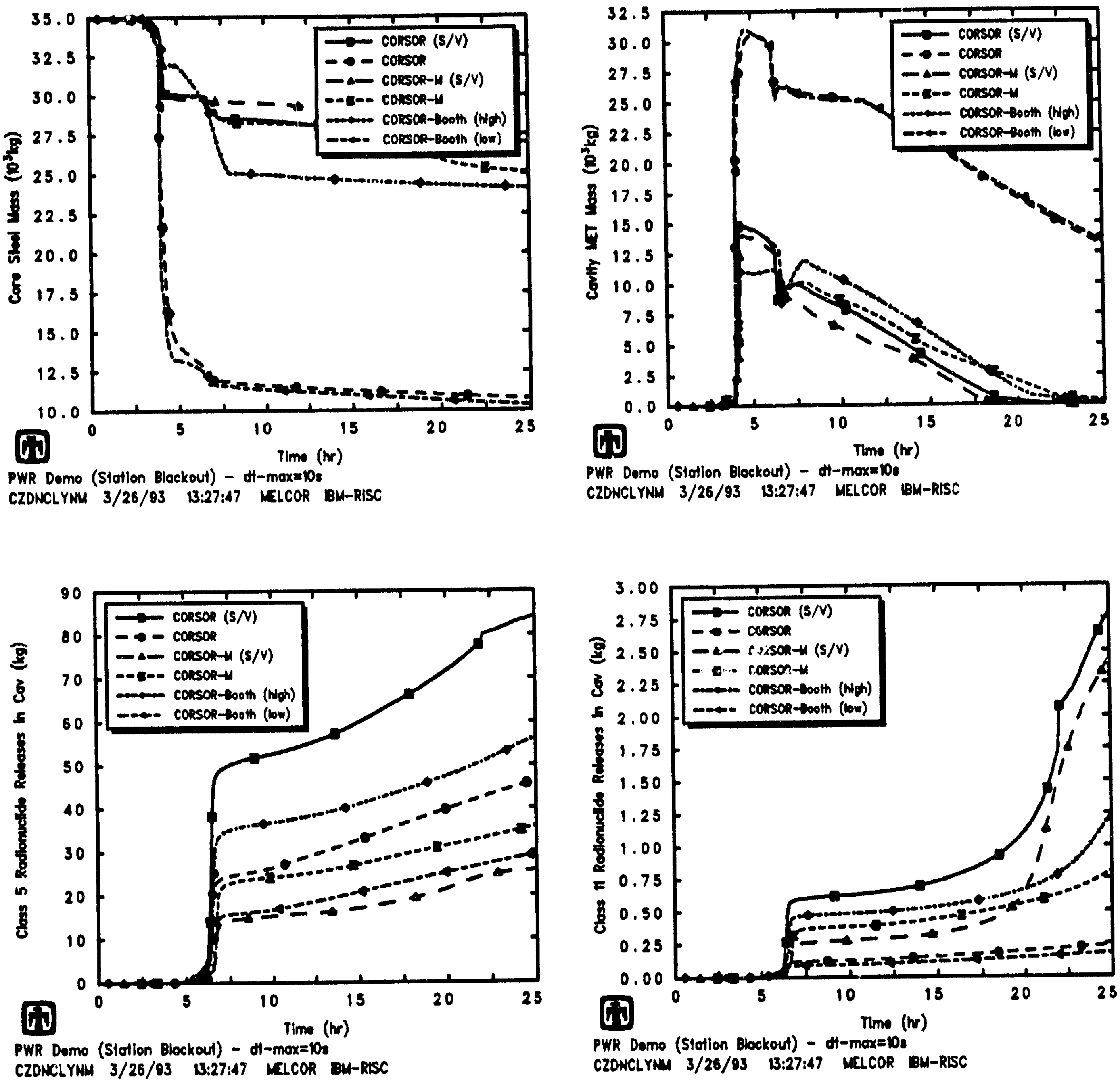

Figure 4.2. Core Steel Masses (upper left), Cavity Metallic Layer Masses (upper right), Class 5 (Te) Releases (lower left) and Class 11 (Sn) Releases (lower right) for Surry TMLB' - CORSOR Options Sensitivity Studies

Sensitivity studies also have been done varying the relative amounts of melt deposited directly in the cavity, in the various containment volume atmospheres, and on various heat structures in the cavity, basement and containment dome. As would be expected, depositing more debris directly into the cavity or onto heat structures reduces the magnitude of the pressure/temperature excursion, while increasing the amount of debris deposited in the containment atmosphere increases the magnitude of the pressure/temperature excursion. In addition, varying the relative amounts of debris deposited into various containment control volume atmospheres changes the relative magnitude of the pressure/temperature excursion predicted: specifying more debris into the cavity atmosphere (a relatively small volume) results in a very large pressure and temperature spike in that local volume, but much smaller pressure/temperature excursions throughout the rest of containment, while specifying more debris into the containment dome atmosphere (a relatively large volume) results in a significantly smaller pressure and temperature spike more uniformly throughout the containment.

Figure 4.3 shows containment dome pressures calculated in several MELCOR DCH sensitivity-study calculations, compared to results from an otherwise equivalent calculation in which the new HPME/DCH model is not used. The upper plot shows the early-time response, around the time of vessel breach, while the lower plot shows the late-time containment pressure response. Calculations are shown with and without HPME/DCH, with and without non-standard hydrogen combustion during HPME/DCH (as discussed in Section 3), and with different debris distributions assumed during HPME/DCH.

Including DCH in the Surry TMLB' analysis also affects the amount of material in the cavity (because some debris settled onto heat structures outside the cavity) and hence the amount of concrete ablated, and affects the source term because release of fission products from airborne debris and from debris settled onto heat structures (instead of into the cavity) is neglected in the MELCOR model.

In response to concerns raised [2] on numeric effects seen in various MELCOR calculations, producing either differences in results for the same input on different machines or differences in results when the time step used is varied, several calculations have been done to identify whether any such effects exist in our Surry PWR TMLB' assessment analyses, and to evaluate their impact on the accident sequence prediction. The reference analysis has been run on a Cray, SUN Sparc2, HP Model 755 and IBM RISC-6000 Model 550 workstations, and on a 50MHz 486 PC, and with the code-selected time step and then the maximum allowable time step set by user input to 5, 2.5 and 1s. Similar, minor differences were found in both numeric studies, including (1) accumulating offsets in both steam generator secondary and pressurizer relief valve cycling early in the transient; (2) timing shifts in clad failure and gap release, and core support plate and lower head penetration failure; (3) variations in amounts of radionuclides released; (4) magnitude and timing offsets in cavity and containment response; and (5) variations in hydrogen burn frequency and duration. However, despite the number of small differences observable, no significant branching into different response modes was found in the time-step or machine-dependency studies. Figure 4.4 presents the primary system and containment pressure history variations calculated during these sensitivity studies.

Note that the differences seen in timing of key events such as clad failure, core plate failure, lower head penetration failure, *etc.*, in these machine-dependency and time-step studies vary by much smaller times (on the order of 10-100s) than the timestep-variation results observed by BNL [19] for their Peach Bottom station blackout analysis with MELCOR 1.8.1 (which often varied by 1,000-10,000s). A large part of this reduction in numeric sensitivity represents the

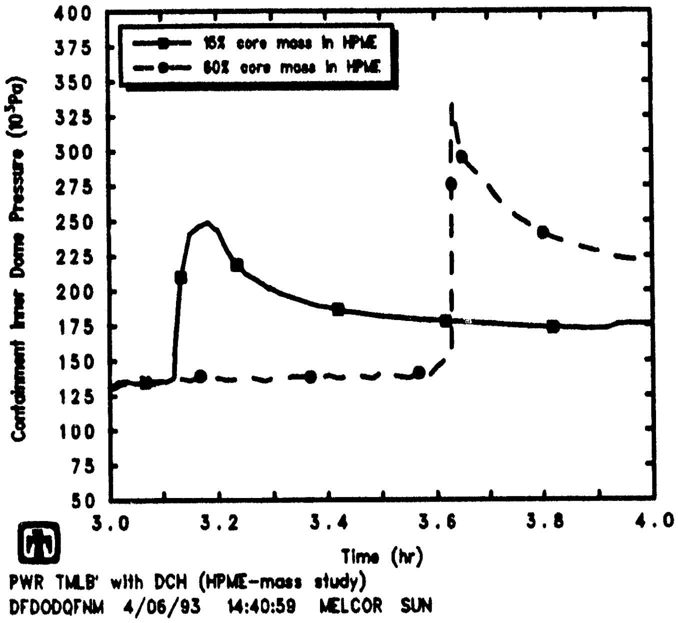

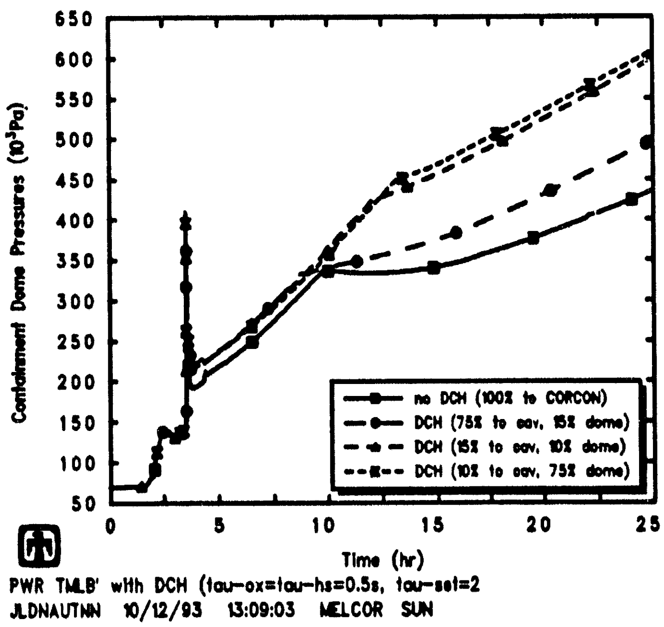

Figure 4.3. Early-Time (top) and Late-Time (bottom) Containment Dome Pressures for Surry TMLB' - HPME/DCH Sensitivity Studies

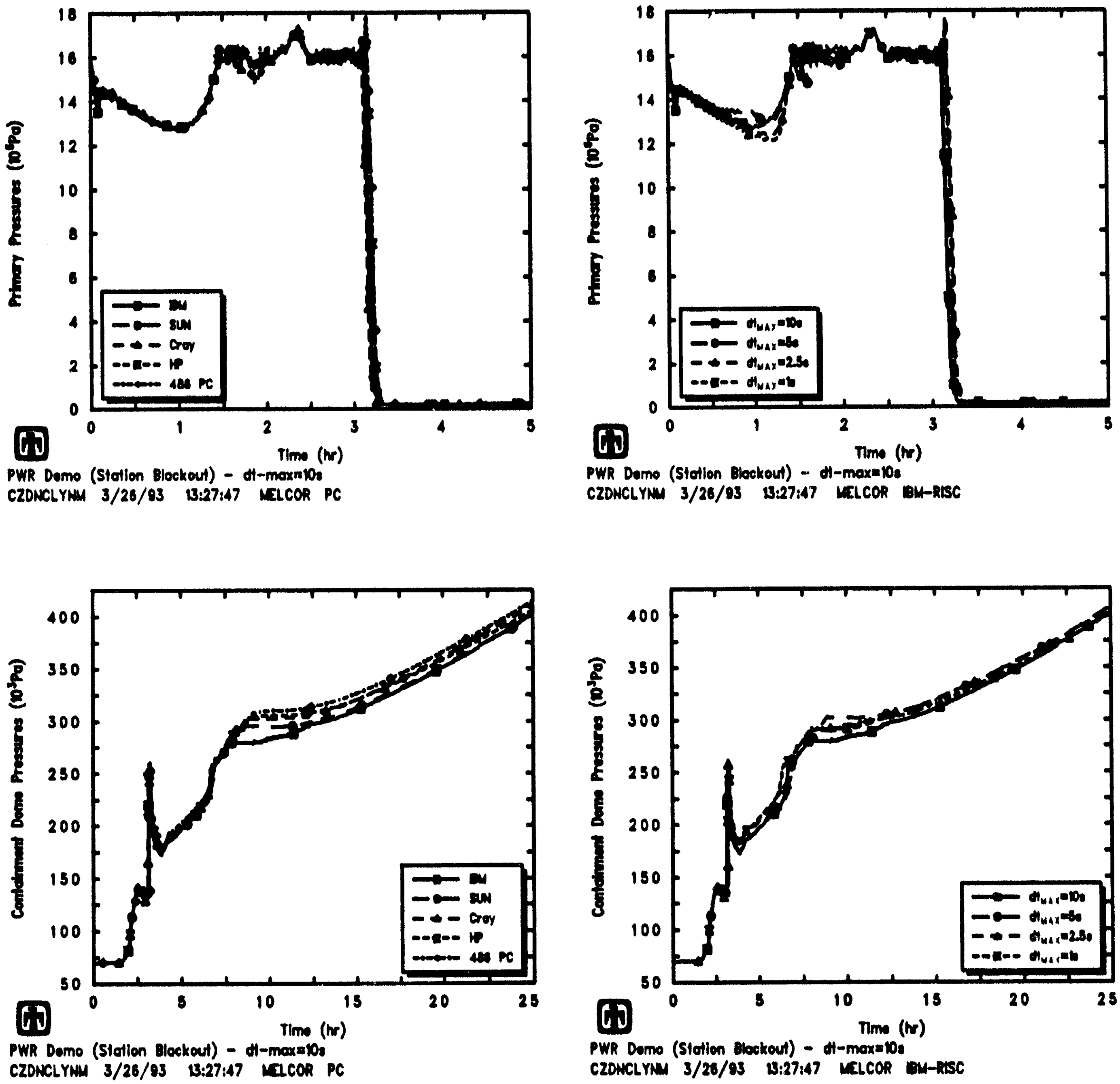

Figure 4.4. Primary System (Top) and Containment (Bottom) Pressures for Surry TMLB' - Machine Dependency (Left) and Time Step (Right) Sensitivity Studies

significant efforts of the code developers since the Peer Review in identifying and eliminating numeric sensitivities in MELCOR. BNL has seen similar significant reduction in time step sensitivity rerunning their Peach Bottom station blackout analysis with MELCOR 1.8.2 [20].

In both the machine-dependency and time-step studies, differences were noted early in the transient in the number of times that the steam generator secondary relief valve and, later, the pressurizer PORV cycled. Those differences were traced to differences in over- and undershooting the valve controller setpoint pressures with different time steps and/or different machine accuracies. The tabular function logic was modified to allow step function input, to minimize valves getting caught in a part-open state interpolating between table entries. A time-step controller has been developed to limit the time step whenever a valve pressure setpoint is being approached, through control function input. Based on prototype testing, this addition to the code's time-step control algorithm will decrease the numeric sensitivity significantly, but some other contributing effect still remain to be identified.

Another numeric effect recently identified in these Surry TMLB' demonstration analyses (in our machine-dependency and time-step sensitivity studies) are differences in the time that hydrogen burns occur in containment, and in the amount of hydrogen burned, which in turn can significantly impact containment failure times and releases to environment. This is currently being investigated.

5 ACRR MP-1 Late Phase Melt Progression Experiment

An assessment of MELCOR is being performed using the MP-1 experiment. These calculations are being performed as post-test analyses, with both test data and the results of other code analyses available for comparison. As part of this assessment, a base case input model is being developed, the results of which will be compared with measured data from the MP-1 experiment [21]. Sensitivity studies will be performed on core (COR), control-volume thermal/hydraulics (CVH) and heat structure (HS) package parameters, and the base case results will be compared with results from the TAC-2D and DEBRIS code models for MP-1.

The purpose of the Melt Progression, or MP, series of experiments was to investigate late phase core melt progression and to obtain data for the benchmarking of severe accident codes for these types of phenomena. The MP-1 experiment was carried out at Sandia National Laboratories in the Annular Core Research Reactor (ACRR) in 1989. This experiment began with an initial configuration representing a degraded core. The fueled portions of the test bundle consisted of three axial regions: a fuel rod region at the bottom, consisting of 32 PWR-type fuel rods; a crust region, containing the 32 fuel rods surrounded by a Zr-ZrO_2-UO_2 crust; and a debris region at the top, consisting of a ZrO_2-UO_2 rubblized debris bed. The debris and crust regions were fully blocked, and the test section was a closed system filled with helium gas at 69kPa (10psi). The MP-1 test bundle was insulated radially and axially to facilitate debris material heatup and melting. The MP-1 experiment used nuclear heating and progressed to partial melting and settling of the debris bed region. No material was melted in the crust region during the experiment.

A new option to initialize core components in a degraded state has been added to the MELCOR code as part of this task. With this new option, the user is allowed to initialize core materials in any state allowed by the MELCOR COR package. In particular, this allows an initial core configuration which contains particulate and conglomerate debris. The base case model for MP-1 uses this new input option for the debris bed and crust regions, respectively.

A preliminary version of the MP-1 base case model has been developed and the results have been compared with experimental data. The base case model consists of three radial rings and 13 axial levels (six debris levels, three crust levels, three stub levels, and one lower plenum level). The debris region initially contains particulate debris composed of ZrO_2 and UO_2 with a particle diameter of 2mm. The crust region is composed of zircaloy-clad fuel rods, modeled as intact components in MELCOR, and conglomerate debris, which resides on the cladding component and which is made up of Zr, ZrO_2 and UO_2. The crust region is initialized in a fully blocked configuration, which is supposed to prevent downward relocation of the particulate debris. The radial and axial insulation layers in MP-1 are represented by multi-layered heat structures in MELCOR. The layers of radial insulation, from the inside out, are thoria (ThO_2), Tantalum (Ta), zirconia (ZrO_2 fiber) and stainless steel. The first three materials are input as new materials, with properties taken from the MP-1 DEBRIS code model [21]; the density and thermal conductivity of UO_2 and stainless steel are also changed to values given in the MP-1 experimental report.

Preliminary results from the MP-1 base case model have been compared with measured temperature histories. Axial temperature profiles at 4800 seconds and 9400 seconds are shown in Figure 5.1. The debris region temperatures at both times corresponds closely with measured data. The crust and stub region temperatures are in fair agreement at 4800 seconds, but diverge from measured data later in the experiment. It appears that the axial temperature profile in lower portions of the test bundle are not captured in the MELCOR results. The radial temperature profiles across the debris region and the radial insulation at 4800 and 9400 seconds are also shown in Figure 5.1. Agreement with measured results is good at both times, except in the outer ZrO_2 layer of the radial insulation. Other codes (DEBRIS and TAC2D) show similar results in this portion of the insulation.

Preliminary sensitivity studies show little or no sensitivity to COR and CVH nodalization, problem time step, or core radiation view factors. Additional sensitivity studies are being performed on COR, CVH and HS package input parameters.

6 Summary and Recommendations

The MELCOR assessment program at Sandia is significantly expanding the available MELCOR validation database. Table 6.1 summarizes the major severe accident phenomenological areas modelled in the MELCOR code, and the MELCOR assessments done at SNL in these various areas. This review of MELCOR verification, validation and assessment to date reveals that most of the severe accident phenomena modelled by MELCOR have received or are receiving some evaluation. Note, however, that in many of these areas the assessment to date does not cover all phenomena of interest, or is based on a limited number of experiments and analyses which may be insufficient to cover the scales of interest and which may be insufficient to allow identification of experiment-specific problems *vs* generic code problems and deficiencies.

The MELCOR code has also been assessed against experiments by a number of other users [22], including BNL (for core damage using the PBF SFD 1-1 and 1-4, and the FLHT-2, -4, and

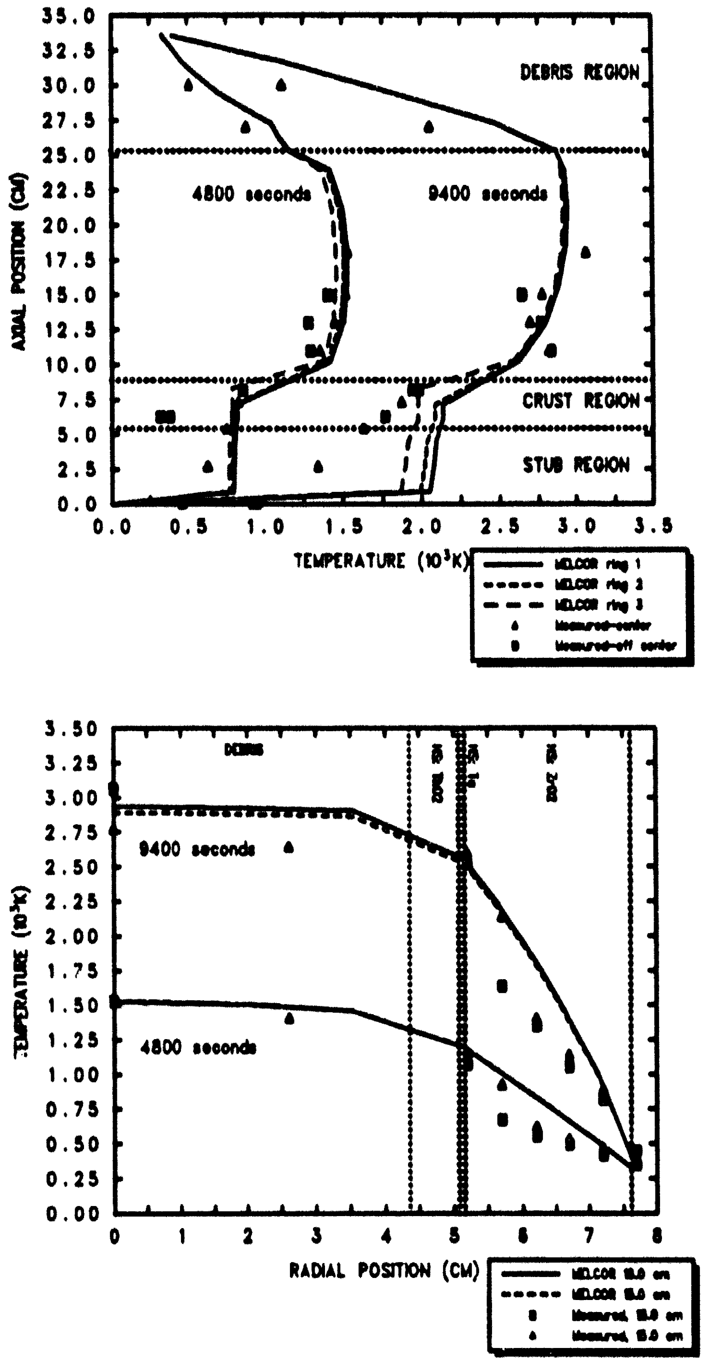

Figure 5.1. MP-1 axial (top) and radial (bottom) temperature profiles for 2 times in the MELCOR calcultion. Radial profiles given for the debris region and include radial heat structure temperatures.

Table 6.1. MELCOR Phenomenological Assessment at SNL

Major Phenomena	MELCOR Packages	Experiments Analyzed
Primary System T/H	CVH,FL,HS	
		OECD LOFT LP-FP-2
		FLECHT SEASET Natural Circulation
In-Vessel Core Damage	COR	
Early-Time (PWR)		OECD LOFT LP-FP-2
Early-Time (PWR)		Phebus B9+ (ISP28)
Early-Time (BWR)		ACRR DF-4
Early-Time (BWR)		CORA 13 (ISP31)
Late-Time		ACRR MP-1
Fission Product Release	RN	
		OECD LOFT LP-FP-2
		ACRR ST-1/ST-2
FP Vapor/Aerosol Transport/Deposition	RN	
Primary System		Marviken ATT-2b/ATT-4
Containment		LACE LA4
Core-Concrete Interaction	CAV	SURC-2
Containment		
T/H	CVH,FL,HS	HDR V44
T/H	CVH,FL,HS	HDR T31.5 (ISP23)
DCH	FDI	SNL/ANL IET
Ice Condenser	HS,RN	PNL 11-6/16-11
Combustion	BUR	(none)
Sprays	SPR	(none)
Integral Behavior	all	
		TMI-2 Standard Problem
		OECD LOFT LP-FP-2
		Surry PWR TMLB'

-5 tests), ORNL (for fission product release using the ORNL VI experiments), UK AEA (for containment thermal/hydraulics using HDR E11.2 (ISP29) and BMC F2), and the University of Madrid (for containment thermal/hydraulics using BMC F2 and DEMONA F2). MELCOR is also being assessed at LANL (for B&W-PWR primary system thermal/hydraulics using several MIST experiments) and at ERI (for BWR primary system thermal/hydraulics using several FIST experiments), for Phebus FPT-0 pretest analyses by several users, and for analysis of the NUPEC hydrogen mixing test ISP35.

There is no experiment (not even the TMI accident) that represents all features of a severe accident (*i.e.*, primary system thermal/hydraulics; in-vessel core damage; fission product and aerosol release, transport and deposition; ex-vessel core-concrete interaction; containment thermal/hydraulics; and hydrogen transport and combustion), and only the TMI accident is at full plant scale. Therefore, it is necessary for severe accident codes to supplement standard assessment against experiment (and against simple problems with analytic or otherwise obvious solutions) with plant calculations that cannot be fully verified, but that can be judged using expert opinion for reasonableness and internal self-consistency (particularly using sensitivity studies) and also can be compared to other code calculations for consistency. In addition to the Surry TMLB' station blackout analysis done at Sandia, there is a large body of plant analyses available, done by various users, and often including extensive sensitivity studies and/or comparisons to other code calculations (*e.g.*, MAAP, SCDAP/RELAP5, THALES-2, STCP) for the same sequences.

Bibliography

[1] R. M. Summers *et al.*,"MELCOR 1.8.0: A Computer Code for Severe Nuclear Reactor Accident Source Term and Risk Assessment Analyses", NUREG/CR-5531, SAND90-0364, Sandia National Laboratories, January 1991.

[2] B. E. Boyack, V. K. Dhir, J. A. Gieseke, T. J. Haste, M. A. Kenton, M. Khatib-Rahbar, M. T. Leonard, R. Viskanta, "MELCOR Peer Review", LA-12240, Los Alamos National Laboratory, March 1992.

[3] L. N. Kmetyk, "MELCOR 1.8.1 Assessment: LACE Aerosol Experiment LA4", SAND91-1532, Sandia National Laboratories, September 1991.

[4] L. N. Kmetyk, "MELCOR 1.8.1 Assessment: FLECHT SEASET Natural Circulation Experiments", SAND91-2218, Sandia National Laboratories, December 1991.

[5] L. N. Kmetyk, "MELCOR 1.8.1 Assessment: ACRR Source Term Experiments ST-1/ST-2", SAND91-2833, Sandia National Laboratories, April 1992.

[6] L. N. Kmetyk, "MELCOR 1.8.1 Assessment: LOFT Integral Test LP-FP-2", SAND92-1373, Sandia National Laboratories, December 1992.

[7] L. N. Kmetyk, "MELCOR 1.8.1 Assessment: Marviken-V Aerosol Transport Tests ATT-2b/ATT-4", SAND92-2243, Sandia National Laboratories, January 1993.

[8] R. J. Gross, "MELCOR 1.8.1 Assessment: PNL Ice Condenser Aerosol Experiments", SAND92-2165, Sandia National Laboratories, August 1993.

[9] L. N. Kmetyk, "MELCOR Assessment at SNL", SAND92-1750C, in Proceedings, 20th Water Reactor Safety Information Meeting, October 1992.

[10] T. J. Tautges, "MELCOR 1.8.2 Assessment: the DF-4 BWR Fuel Damage Experiment", SAND93-1377, Sandia National Laboratories, October 1993.

[11] L. N. Kmetyk, "MELCOR 1.8.2 Assessment: IET Direct Containment Heating Experiments", SAND93-1475, Sandia National Laboratories, October 1993.

[12] L. N. Kmetyk, "MELCOR 1.8.2 Assessment: Surry PWR TMLB' (with a DCH Study)", SAND93-1899, Sandia National Laboratories, to be published.

[13] E. A. Boucheron and J. E. Kelly, "MELCOR Analysis of the Three Mile Island Unit 2 Accident", Nuclear Technology 87, December 1989.

[14] G. M. Martinez, "MELCOR Post-Test Calculations of the HDR Experiment", letter report to R. B. Foulds, NRC, September 29, 1989.

[15] G. M. Martinez, "MELCOR Calculations of ISP28 SFD PHEBUS Test B9+", Letter report to B. Adroguer, CEN/Cadarache, France, dated December 14, 1990.

[16] G. M. Martinez, "MELCOR Calculations of ISP28 SFD PHEBUS Test B9+", Letter report to F. Eltawila, NRC, dated December 20, 1991.

[17] R. J. Gross, S. L. Thompson, G. M. Martinez, "MELCOR 1.8.1 Calculations of ISP 31: the CORA13 Experiment", SAND92-2863, Sandia National Laboratories, June 1993.

[18] D. A. Powers, J. E. Brockmann, A. W. Shiver, "VANESA: A Mechanistic Model of Radionuclide Release and Aerosol Generation during Core Debris Interactions with Concrete". NUREG/CR-4308, SAND85-1370, Sandia National Laboratories, July 1986.

[19] I. K. Madni, "MELCOR Simulation of Long-Term Station Blackout at Peach Bottom", NUREG/CP-0113, Proceedings, 18th Water Reactor Safety Information Meeting, Gaithersburg MD, October 1990.

[20] I. K. Madni, "Analyses of Long-Term Station Blackout Without Automatic Depressurization at Peach Bottom Using MELCOR", NUREG/CR-5850, BNL-NUREG-52319, Brookhaven National Laboratory, to be published.

[21] R. D. Gasser, R. O. Gauntt, S. Bourcier, "Late Phase Melt Progression Experiment – MP-1", NUREG/CR-5874, SAND92-0804, Sandia National Laboratories, to be published.

[22] L. N. Kmetyk, "Survey of MELCOR Assessment and Selected Applications", SAND92-1273, Sandia National Laboratories, to be published.

DATE
FILMED
1 / 21 / 94

END